ELSEVIER

Brain Research Bulletin 67 (2005) 403–412

BRAIN RESEARCH BULLETIN

www.elsevier.com/locate/brainresbull

Variants of uncertainty in decision-making and their neural correlates

Kirsten G. Volz *, Ricarda I. Schubotz, D. Yves von Cramon

Max Planck Institute for Human Cognitive and Brain Sciences, P.O. Box 500 355, D-04303 Leipzig, Germany

Available online 7 July 2005

Abstract

When leaving the tidy world of rules and people start judging probabilities on an intuitive basis, it revealed that they have some intuitions to choose from. One could refer to them as a family of subjective probability concepts or following Kahneman and Tversky, as variants of uncertainty. The authors distinguished between external and internal attributions of uncertainty and could show that the perceived reason of uncertainty determines the selected coping strategy. To investigate whether variants of uncertainty can also be distinguished on the cerebral level, two functional magnetic resonance imaging studies were conducted. Participants had to predict events (abstract visual stimuli) under parametrically varying degrees of (un-)certainty. In the first experiment, uncertainty was induced by the manipulation of event probability (externally attributed uncertainty). In the second experiment, uncertainty depended on participants' knowledge of valid rules of event occurrence, as trained before the experimental session (internally attributed uncertainty). As a result, parametric analyses revealed that activation within the posterior fronto-median cortex, particularly within mesial Brodmann area (BA) 8, increased with increasing uncertainty, no matter for which reason uncertainty emerged. Furthermore, it was found that different variants of uncertainty entailing different coping strategies can be dissociated due to additionally activated networks. Concluding, increasing activation within mesial BA 8 reflects that we are uncertain, additional networks what we do to resolve uncertainty in order to achieve future rewards. Hence, the phenomenological distinction between processes related to externally and internally attributed uncertainty is paralleled on the cerebral level.

Keywords: Decision-making; Prediction; fMRI; Posterior fronto-median cortex

1. Introduction

Interest in understanding the neurobiological mechanisms by which decisions are made has grown just recently. Such different disciplines like economics, psychology and neuroscience joint together in order to attempt a unified explanation of decision-making [23]. Yet, at that time, we are far away from providing a single general theory of human decision-making. But incorporating and bringing together the findings from the different disciplines concerning different aspects of decision-making will help in understanding the big picture. To keep in view with this aim, the present study deals with one aspect of decision-making, namely with the cerebral correlates of processes related to different variants of uncertainty.

In decision-making, it is rather important to anticipate consequences associated with different options or actions in order to decide favorably. However, there are events and circumstances in life that influence the outcome of decisions therewith making decisions uncertain. Uncertainty-causing events can be externally originating in the social and natural environment as well as internally originating within the individual. Kahneman and Tversky [30] discriminated variants of uncertainty subject to the perceived cause of uncertainty, i.e., externally attributed uncertainty and internally attributed uncertainty. The authors sub-divided the former into uncertainty based on frequencies and uncertainty based on propensities, the latter into uncertainty based on arguments and uncertainty based on introspective confidence, i.e., knowledge. Kahneman and Tversky [30] could show that the perceived cause of uncertainty is reflected in the

* Corresponding author. Tel.: +49 341 9940 134/221; fax: +49 341 9940 134/221.
E-mail address: volz@cbs.mpg.de (K.G. Volz).
URL: http://www.cbs.mpg.de.

0361-9230/$ – see front matter © 2005 Elsevier Inc. All rights reserved.
doi:10.1016/j.brainresbull.2005.06.011

way subjects try to resolve their uncertainty. A prominent coping strategy with uncertainty of frequency is to try to rate the probability of external events (e.g., "there is a 60% chance for rain tomorrow"). In contrast, a successful coping strategy with uncertainty of knowledge is an intensive memory search, most likely in combination with the attempt to get missing information from valid external sources (e.g., "I am quit sure that possums are mammals, but I do not know exactly"). That way, strategic processes are taken to reflect the respective variant of uncertainty. By using functional magnetic resonance imaging (fMRI), the brain may serve as an external criterion to test whether the phenomenological distinction drawn by Kahneman and Tversky [30] and several other researchers (e.g., [4,28,48]) is paralleled on the cerebral level.

Accordingly, by using fMRI, we aimed to investigate the neural correlates of processes related to externally attributed uncertainty in Experiment 1 (Exp. 1) and processes related to internally attributed uncertainty in Experiment 2 (Exp. 2) and beyond in as much the latter differ from those induced by externally attributed uncertainty. To reliably detect areas systematically varying with the level of the respective variant of uncertainty, we induced different degrees of uncertainty in the respective experiment, i.e., a parametric manipulation.

To date, there is a great number of studies investigating brain activations induced by uncertainty-related paradigms including rule induction and application [24], inductive reasoning [25], hypotheses testing [12], anticipation of monetary gains and losses [3,32], response conflict (e.g., [50]), dynamical motion predictions [50] or guessing [13,15]. Common to all these paradigms, is the prediction of uncertain events. The neural correlates reported with uncertainty are posterior fronto-median areas, including mesial Brodmann area (BA) 8, anterior mesial BA 6, corresponding to the pre-supplementary motor area (pre-SMA) and BA 32 often in company with BA 24, usually referred to as the dorsal anterior cingulate cortex. By contrasting rule learning with item learning, inductive reasoning with deductive reasoning, hypothesis testing with response selection, response conflict with no conflict or guessing with reporting, these studies suggest a general difference between processes under uncertainty and those which are quite certain. However, from where the uncertainty arises is neglected so far.

By using a parametric approach, we investigated whether processes related to the different variants of uncertainty are reflected by fronto-median activations (main effects) and if so, whether this brain activation also increases with increasing uncertainty (parametric effects). In a subsequent group comparison (between-subjects design), it was investigated whether networks underlying externally and internally attributed uncertainty differ significantly. Particularly, since storage and retrieval of acquired visuomotor associations are required for the suggested coping strategy in decisions under internally attributed uncertainty [30], fronto-parietal activations were expected in networks that sub-serve working memory functions [39,17].

In addition to fronto-median areas orbito-frontal areas are known to be engaged in uncertain decisions, particularly those that are induced by reward expectancy [3,9,38,43]. However, due to technical restrictions of the T_2^* sequence in a 3T NMR system that usually causes signal voids [37], medial orbito-frontal activations could not be detected in the present experiments.

2. Materials and methods

2.1. Participants

Sixteen (five females, mean age 24.9 years, range 21–35 years) right-handed, healthy volunteers participated in Exp. 1 and 12 volunteers (seven females, mean age 25.1, range 20–31 years) in Exp. 2. Informed consent was obtained from each participant according to the declaration of Helsinki. Experimental standards were approved by the local ethics committee of the University of Leipzig. Data were handled anonymously.

2.2. Stimuli, task and experimental session

Stimuli consisted of comic pictures showing UFOs differing either in color, shape or figurative content (see Fig. 1). Four different colors, shapes and comic figures were employed, respectively. Within each trial, two UFOs were concurrently presented, one on the right and one on the left side of the screen (degrees of visual angle: 2.0). Participants had their index fingers on a left and a right response button, spatially corresponding to the stimulus locations on the screen. One pair of UFOs was presented for 2 s during which participants' response was recorded, subsequently, a feedback was presented for 1.5 s. The experimental session was designed such that participants were presented with blocks of five trials of the same experimental condition, which was announced by a verbal task cue of 5 s in Exp. 2 and by the presentation of a fixation cross of 5 s in Exp. 1. The inter-block-intervals were 5 s and these also constituted the non-events. In Exp. 1, 10 blocks were presented for each of the five experimental conditions and the control condition, resulting in 60 blocks or 300 trials altogether. In Exp. 2, 15 blocks were presented for each of the four experimental conditions and 12 blocks for the control condition, resulting in 72 blocks or 360 trials altogether. Blocks were presented in randomized order and the order was balanced between participants. An enhancement of the BOLD signal was achieved by employing a jittering which allowed the assessment of the BOLD-response at different times relative to the event onset. Both the beginning of each block as well as the inter-trial-interval were jittered. Accordingly, while trial duration (3.5 s) and trial onset asynchrony (5 s) were kept constant, the inter-trial-interval (mean duration of 1.5 s) varied by a jittering of 0, 500, 1000 or 1500 ms, respectively, assigned randomly to the trials.

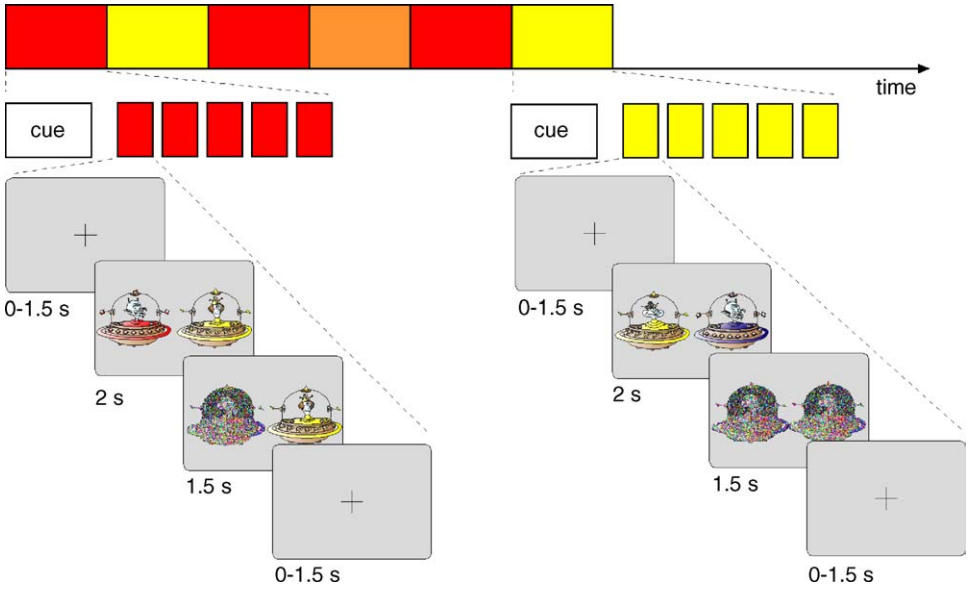

Fig. 1. Example of the stimulation: In Exp. 1 and in Exp. 2 blocks with different experimental conditions (color-coded) were presented in randomized order. One block consisted of a cue and five trials of the same experimental condition. Stimuli were presented for 2 s during which participants' response was recorded followed by a feedback of 1.5 s. On the left panel, a positive feedback is shown, on the right, panel a negative.

Both in Experiments 1 and 2 participants', task was to predict which of the two concurrently presented UFOs would win in a virtual competition game. When a new stimulus pair came up, participants were instructed to press the response button spatially corresponding to the UFO, they excepted to win. The response phase was restricted to the presentation time of the stimuli, i.e., 2 s. Feedback showing a masking of both UFOs indicated that one decided in favor of the loser, whereas the presentation of the chosen UFO and a masking of the other one indicated that one decided in favor of the winner. The feedback following late responses (time outs) was identical to the negative feedback, i.e., both stimuli masked.

Uncertainty of frequency in Exp. 1 was manipulated by varying the winning probabilities between the experimental conditions (ranging from 60 to 100%). Winning probabilities depended on the specific pairing of stimuli. Participants were instructed to exclusively attend to the figure dimension, whereas the stimulus properties color and shape varied randomly across figures. Six possible figure-pairings were generated by combining the four different figures (e.g., A–B, A–C, A–D, B–C, B–D and C–D). Five of these pairings were associated with a particular winning probability, which was calculated across the entire experimental session. The associations between figure-pairing and winning probability were unchanged throughout the experiment. Accordingly, depending on the figure-pairing feedback showed one figure with a mean probability of .6 (that D wins against C), .7 (that D wins against B), .8 (that B wins against C), .9 (that C wins against A) and 1.0 (that A wins against D), respectively. The remaining figure-pairing (A–B) was used as control condition in which three arrows indicated the winning stimulus and participants were asked to chose this very one. The three arrows pointed equally often to one of the two stimuli, i.e., A won against B with a probability of .5. Average winning probabilities were almost balanced between the four figures (A: .533, B: .533, C: .500 and D: .433). By balancing the probabilities in this way, it was aimed to avoid cross-talk between pairings and subsequent effects like latent inhibition to operate between blocks.

To allow for a comparison between Exps. 1 and 2, we used the same stimulus material and modified only a few features of the experimental paradigm, i.e., the manipulation of uncertainty and the announcement of experimental conditions by verbal task cues in Exp. 2. Uncertainty of knowledge was manipulated by varying the degree of knowledge that participants were provided with regarding the winning rules, each of which determining a 100% winning probability as depending on stimulus features. Within each stimulus dimension (color, shape, figure) five possible pairings were generated by combining the four different values (e.g., within the color dimension: red-yellow, red-blue, yellow-blue, yellow-green and blue-green). The sixth pairing (e.g., red-green) was generally skipped to restrict rule complexity. Each of the three stimulus dimensions represented a rule group consisting of five different sub-rules specifying the correct feedback. The resulting 15 rules were valid throughout the entire experimental session (e.g., yellow always trumped blue). To induce different levels of uncertainty of knowledge, participants were provided with different amounts of information concerning the 15 winning-rules; one rule group was trained up to optimal performance prior to the fMRI session (trained rules condition). A second rule group was verbally instructed at the end of this training session, but not practiced (learned

rules condition). The third rule group was neither trained nor verbally instructed, so that participants were initially ignorant about this set of rules (explored rules condition). In a fourth condition, participants were asked to test which one out of two rule groups, i.e., the trained or the learned rule group was valid within a given block (tested rules condition). The assignment of stimulus dimension to rule group was balanced between participants. Parallel to Exp. 1, participants' task in the experimental conditions as well as in the control condition was to predict which UFO would win in a virtual competition game, whereas in the control condition, the winning stimulus was indicated by three arrows.

2.3. Imaging

Imaging was performed at 3 T on a Bruker Medspec 30/100 system equipped with the standard bird cage head coil. Slices were positioned parallel to the bi-commissural plane (AC–PC) with 16 slices (thickness 5 mm, spacing 2 mm) covering the whole brain. A set of 2D anatomical images was acquired for each participant immediately prior to the functional experiment, using a MDEFT sequence (256 pixel × 256 pixel matrix). Functional images in plane with the anatomical images were acquired using a single-shot gradient EPI sequence (TE = 30 ms, 64 pixel × 64 pixel matrix, flip angle 90°, field of view 19.2 cm) sensitive to BOLD contrast. During each trail, 2 images were obtained from 16 axial slices at the rate of 2.5 s. In a separate session, high-resolution whole brain images were acquired from each participant to improve the localization of activation foci using a T_1-weighted 3D-segmented MDEFT sequence covering the whole brain.

2.4. Data analysis

The MRI data were processed using the software package LIPSIA [34]. Functional data were corrected for motion artifacts using a matching metric based on linear correlation. To correct for the temporal offset between the slices acquired in one scan, a sinc-interpolation was applied. A temporal high-pass filter with a cut-off frequency with 1/170 Hz was used for baseline correction of the signal and a spatial Gaussian filter with 5.65 mm FWHM was applied. The anatomical slices were co-registered with the full brain scan that resided in the stereotactic coordinate system and then transformed by linear scaling to a standard size. The transformation parameters obtained from this step were subsequently applied to the functional slices so that the functional slices were also registered into the stereotactic space. Slice-gaps were scaled using a trilinear interpolation, generating output data with a spatial resolution of 3 mm × 3 mm × 3 mm (27 mm^3).

The statistical evaluation was based on a least-squares estimation using the general linear model (GLM) for serially autocorrelated observations (random effects model; [18,19,55]). An event-related design was implemented, i.e., the hemodynamic response function was modeled by means of the experimental conditions for each stimulus (event = onset of stimulus presentation). The design matrix was generated utilizing a synthetic hemodynamic response function and its first and second derivative [20] and a response delay of 6 s. The model equation including the observation data, the design matrix and the error term was convolved with a Gaussian kernel of dispersion of 4 s FWHM to deal with the temporal autocorrelation [55]. Contrast images, i.e., estimates of the raw-score differences between specified conditions were generated for each subject. The single subject contrast images entered into a second-level random effects analysis for each of the contrasts. The group analysis consisted of a one-sample *t*-test across the contrast images of all subjects that indicated whether observed differences between conditions were significantly different from zero. Subsequently, *t*-values were transformed into *Z*-scores. To protect against false positive activations, only regions with *Z*-score greater than 3.1 ($p < 0.001$; uncorrected) and with a volume greater than 225 mm^3 (5 voxels) were considered.

Effects of increasing externally and internally attributed uncertainty were analyzed by using a parametric design [5,6]. So as to model the effects of uncertainty independent from the cause but as a measure of performance, a regressor was used that consisted in the group-averaged error per experimental condition. That is, the average error for the conditions $p = .6$, .7, .8, .9 and 1.0 in Exp. 1 and trained, learned, explored and tested in Exp. 2. This regressor is referred to as "condition-regressor" in the following. In both experiments, the condition-regressor referred to trials of all uncertain experimental conditions, but not of the control condition. The latter, which were certain predictions were modeled as a separate onset vector within the same model. To control for slow attenuation effects over the course of the experimental session, including the reduction of condition-independent uncertainty, a second "attenuation-regressor" was implemented in the same model within each parametric analysis. In both experiments, the attenuation-regressor consisted in the group-averaged error per trial. Statistical independence of the condition- and the attenuation-regressor in each experiment was achieved by balancing the order of conditions in a way that the group-averaged event probability was .80 at each trial in Exp. 1 and that the distributions of all knowledge levels was equal in Exp. 2.

Contrast maps per experiment were generated that extracted following effects of interest independently from each other; first, the main task effects were investigated by building the contrast between all collapsed experimental conditions and the control condition. Second, the parametric effects of levels of uncertainty were tested by using the respective condition-regressor. Third, to investigate whether brain areas associated with processes related to externally attributed uncertainty differed significantly from those associated with processes related to internally attributed uncertainty contrast images were compared voxelwise using a two-sample *t*-test.

Table 1
Error rates (%) and reaction times (ms) are shown for the different conditions in Exp. 1 ($n = 16$) and Exp. 2 ($n = 12$)

	Error rates		Reaction times	
	Mean	S.D.	Mean	S.D.
Experiment 1				
$p = 1.0$	14.3	7.8	997.5	125.2
$p = .9$	29.4	9.2	1004.9	150.7
$p = .8$	41.2	8.2	1026.0	177.8
$p = .7$	47.2	9.7	1030.4	168.6
$p = .6$	52.5	3.8	1095.5	153.7
Control	0	0	932.0	203.5
Experiment 2				
Trained	6.6	6.9	881.2	149.4
Learned	15.7	12.5	901.2	228.3
Explored	16.8	6.8	878.6	185.4
Tested	23.4	13.8	1005.2	198.9
Control	0	0	617.8	95.3

3. Results

3.1. Behavioral results

Performance was measured by the rate of erroneously answered trials and reaction times of correctly answered trials (see Table 1). In Exp. 1, a repeated measures ANOVA with the five-level factor UNCERTAINTY yielded a significant main effect for both error rates ($F(4,60) = 54.5$; $p < .0001$) and reaction times ($F(4,60) = 6.0$; $p < .001$). A reduction of condition-independent uncertainty over the course of the experimental session was indicated by a significant decrease in reaction times ($F(3,45) = 15.4$; $p < .001$) well as by a significant decrease in error rates ($F(3,45)=2.93$; $p = .04$). In Exp. 2, a repeated measures ANOVA with the four-level factor UNCERTAINTY yielded a significant main effect for error rates ($F(3,36) = 14.0$, $p < .0001$) but not for reaction times ($F(3,36) = 2.2$, $p = .11$). Slow unspecific attenuation effects due to a reduction of condition-independent uncertainty were indicated by a significant decrease in reaction times over the course of the experimental session ($F(3,33) = 3.7$; $p = .02$) but not by a decrease in error rates ($F(3,33) = 1.0$; $p = .39$). Errors dropped from the first to the last quartile by 4.7%, as compared to 5.5% in Exp. 1.

4. MRI data

4.1. Main task effects of externally and internally attributed uncertainty

When testing for the main task effect in Exp. 1 significant activations were elicited within the right posterior fronto-median cortex (pFMC), particularly within mesial BA 8/6, the right anterior insula, the cuneus, the cerebellar vermis extending laterally into the paramedian portion of the left cerebellar hemisphere and within a sub-cortical network, including the ventral striatum, the thalamus and the right mid-brain area (see Fig. 2 and Table 2). Testing for the main task effect in Exp. 2 significant activations were elicited within the right pFMC, particularly within mesial BA 8, bilaterally within inferior pre-frontal areas (inferior frontal junction area (IFJ), i.e., at the cross-section of the inferior frontal sulcus and the inferior pre-central sulcus), midportions of the middle frontal gyrus (MFG) along the inferior frontal sulcus (IFS), the antero-superior insula, posterior parietal cortices (along the banks of the intraparietal sulcus (IPS)), within pretectal areas, and extrastriate visual cortices (see Fig. 2 and Table 2).

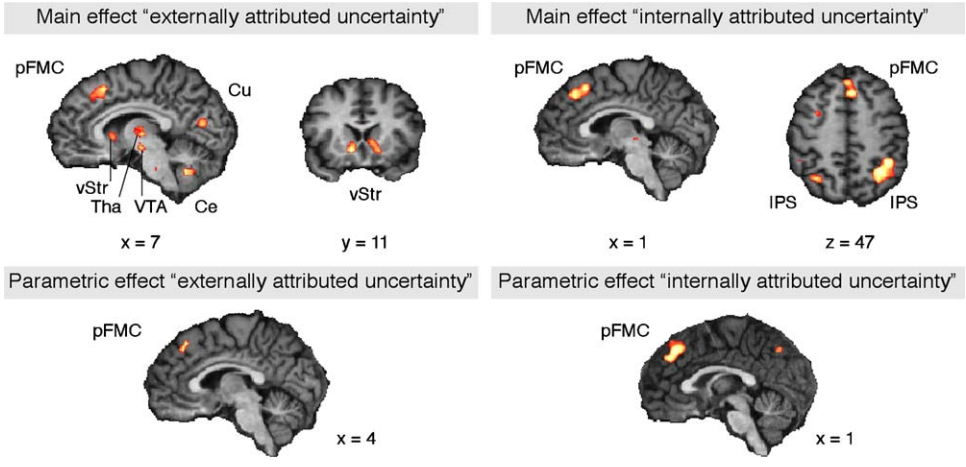

Fig. 2. Results of the main task effects as well as of the parametric effects of externally and internally attributed uncertainty ($Z > 3.09$). Group-averaged activations are shown on sagittal, axial and medial slices of an individual brain normalized and aligned to the Talairach stereotactic space (for activation coordinates, see Tables 2 and 3). *Abbreviations:* pFMC, posterior fronto-median cortex; Ce, cerebellum; Cu, cuneus; IPS, intraparietal sulcus; Tha, thalamus; vStr, ventral striatum.

Table 2
Anatomical specification, Talairach coordinates (x, y, z) and maximal z-scores (Z) of significantly activated voxels in uncertain decisions (all levels collapsed) in contrast to the control condition

Area	Talairach coordinates			
	x	y	z	Z
Main effect (Experiment 1)				
Posterior fronto-median cortex (BA 8/6)	8	18	46	4.4
Ventral striatum	−12	12	−3	4.5
	21	15	−6	4.0
Thalamus	−15	−18	12	3.4
	8	−17	6	4.2
Midbrain area	8	−17	−6	3.9
Anterior insula	40	19	6	4.1
Cerebellum	1	−68	−23	4.7
Cuneus	4	−71	14	4.1
Main effect (Experiment 2)				
Posterior fronto-median cortex (mesial BA 8)	4	21	47	4.5
Posterior fronto-median cortex (anterior BA 8)	1	33	41	4.2
Inferior frontal junction area	−38	9	32	3.8
	40	13	32	3.7
Middle frontal gyurs	−44	25	23	4.4
	37	27	26	4.4
Antero-superior insula	−26	24	6	4.5
	28	22	9	4.0
Intraparietal sulcus	−26	−62	50	3.8
	31	−53	47	4.6
Pretectal area	−5	−29	0	3.8
	4	−26	0	3.3
Extrastriate visual cortex	−35	−54	−9	4.3
	31	−50	−8	4.3

4.2. Parametric effects of externally and internally attributed uncertainty

When testing for the parametric effect of externally attributed uncertainty positively co-varying voxels were found to be located within the right pFMC, particularly within mesial BA 8, the right thalamus, the right anterior insula and the left cerebellar cortex (see Fig. 2 and Table 3). When testing for the parametric effect of internally attributed uncertainty positively co-varying voxels were found to be located within the fronto-median cortex (anterior portion of mesial BA 8), the left IJF, the right midportion of MFG and bilaterally within posterior parietal cortices along the banks of the anterior portion of the IPS (see Fig. 2 and Table 3).

4.3. Comparison between externally and internally attributed uncertainty

To investigate whether networks underlying externally attributed uncertainty differ significantly from those underlying internally attributed uncertainty a between-subjects group comparison was calculated using a two-sample t-test, i.e., the two sets of contrast images from Exps. 1 and 2 were compared voxelwise [34]. According to the initial hypothesis, it was focused on three regions of interest: pFMC, fronto-lateral and posterior parietal areas. As expected, the inferior frontal cortex (IFJ bilaterally; midportion of left MFG/IFS) and posterior parietal cortices correlated positively with uncertainty when internally attributed. Talairach coordinates were nearly identical to coordinates of the main effect (see Table 3). The number of significantly activated voxels indicating a difference within the anterior portion of mesial BA 8 was negligible (11 voxels) and restricted to the most anterior part of this region.

Table 3
Anatomical specification, Talairach coordinates (x, y, z) and maximal z-scores (Z) of voxels co-varying positively with increasing uncertainty (parametric effects) and of voxels indicating the degree of significance of the group difference for internally attributed uncertainty (group comparison)

Area	Talairach coordinates			
	x	y	z	Z
Parametric effect (Experiment 1)				
Posterior fronto-median cortex (BA 8)	4	30	46	3.9
Thalamus	8	−11	9	3.4
Anterior insula	37	12	−3	3.6
Cerebellum	−18	−71	−29	4.0
Superior frontal sulcus	17	3	46	3.6
Middle frontal gyurs	37	21	36	3.7
Inferior parietal lobule	46	−53	38	4.0
Parametric effect (Experiment 2)				
Posterior fronto-median cortex (BA 8)	1	33	41	4.3
Inferior frontal junction area	−44	12	38	4.0
Middle frontal gyurs	40	24	35	4.2
Inferior parietal sulcus	−38	−42	44	4.1
	40	−53	50	4.2
Group comparison (Experiment 1 vs. Experiment 2)				
Posterior fronto-median cortex (anterior BA 8)	−2	31	47	4.0
Inferior frontal junction area	−41	18	35	4.2
	40	13	32	3.8
Middle frontal gyurs	−41	25	23	4.2
Inferior parietal sulcus	−29	−62	50	3.8
	−47	−44	50	4.0
	31	−53	47	4.7

5. Discussion

Experiment 1 as well as Experiment 2 were designed to investigate whether processes related to different variants of uncertainty are reflected within the same brain areas. By using a parametric approach and therewith inducing different degrees of uncertainty, it was aimed to identify and compare the brain correlates of processes related to externally

attributed uncertainty (Exp. 1), i.e., uncertainty of frequency, with those of processes related to internally attributed uncertainty, i.e., uncertainty of knowledge (Exp. 2).

As a common cortical substrate of uncertain predictions, regardless of uncertainty attribution, mesial Brodmann area 8 was found to be significantly activated. Moreover, this area revealed to vary systematically with the degree of uncertainty such that the more uncertain a decision the more activation within mesial BA 8 was found. In contrast, activation within other brain areas differed significantly between the two variants of uncertainty such that internally attributed uncertainty specifically engaged a fronto-parietal network bilaterally. Important to note is that slow attenuation effects did not distort the activation pattern we were interested in as the reduction of condition-independent uncertainty over the course of the experiment draws on different, non-overlapping brain areas.

5.1. Attribution-independent activation of uncertainty: mesial BA 8

To date, activation within mesial BA 8 has been found to be involved in a number of studies investigating uncertainty-related paradigms. However, activation within adjacent mesial areas BA 6 and BA 32/24 has also repeatedly found in tasks that induce uncertainty. Although research on the anatomical and functional organization of the pFMC has just recently begun, in light of the existing literature there seems evidence for a functional dissociation, namely between mesial BA 8 and BA 32/24 (see Fig. 3). This view is supported by cytoarchitectonic differences between these two areas. Mesial BA 8 is a granular pre-frontal isocortex, whereas BA 32/24 can be sub-divided into agranular (BA 24) and dysgranular (BA 32) cortex. Since it is widely accepted that laminar differentiations reflect functional differentiations of the cortex, it is suggested that activation within mesial BA 8 on the one hand and activation within BA 32/24 (often in company with pre-SMA) on the other are preferentially engaged in different decisions under uncertainty such that the former is elicited by decision conflicts, whereas the latter is elicited by response conflicts.

Studies reporting activation within BA 32/24 often in combination with mesial BA 6 typically employ paradigms that can be described by the following aspects: (a) SR-rules are simple (one-to-one) mappings, often spatially compatible and usually, instructed, respectively, known beforehand; (b) two response tendencies are activated concurrently, so that conflict arises on the response level; (c) errors are usually induced by time pressure and/or perceptual difficulty; (d) conflicts could be diminished by a close stimulus inspection; (e) feedback evaluation allows to improve performance in perceptual and motor skills. Exemplifying are paradigms like the Eriksen flankers task, its modifications, go/no-go tasks or the Stroop task and its variations (e.g., [8,21,22,31,44,50,51]). Common to all these paradigms is the manipulation that the stimulus primes a pre-potent but incorrect response. At the same time, subjects know which stimulus–response–association will result in an error or in a reward.

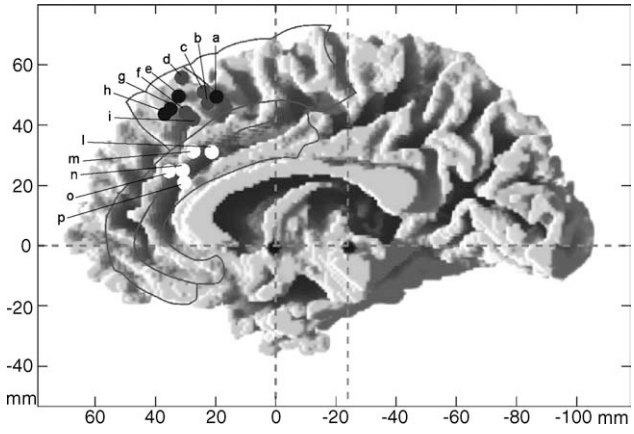

Fig. 3. Comparison between fronto-median activations of Exp. 1 (a and e), Exp. 2 (g and h), and those of other studies on decisions under uncertainty. The right fronto-median wall of a white matter-segmented individual brain is shown from the midline. The outer frame shows coordinates from Talairach and Tournoux [47]. The cross-hairs are cut through the anterior and the posterior commissure (AC–PC), with vertical orientation lines (VAC–VPC) perpendicular to AC–PC, respectively. BA 6, 8, 24 and 32 are outlined. Light and dark gray spheres refer to activation foci within mesial BA 8, white spheres to those within BA 32/24. Spheres a and g correspond to the main task effects of Exps. 1 and 2; spheres e and g correspond to the parametric effects of increasing uncertainty in Exps. 1 and 2. Other letters and spheres correspond to the following studies: (b) Schubotz and von Cramon [46] (prediction difficulty); (c) Elliott and Dolan [12] (hypothesis testing); (d and g) Goel and Dolan [24] (rule application); (f) Ullsperger and von Cramon [49] (response competition); (l) Ullsperger and von Cramon [50] (error detection); (m) Elliott and Dolan [12] (committing oneself to choice); (n) Critchley et al. [9] (uncertainty and arousal); (o) Elliott et al. [15] (guessing); (p) Rogers et al. [43] (risky choice).

Just recently, a differential engagement of BA 6 and BA 32/24 has been suggested such that BA 32/24 is predominantly reported in error monitoring [7,22,50], whereas BA 6 is mainly found with conflict detection [45,50]. The assumption that these two sub-processes can be stressed by contrast building was confirmed by a meta-analysis by Fassbender et al. [16].

In contrast, studies reporting activation within mesial BA 8 (in the absence of BA 32/24 activation) typically employ paradigms that can be described by the following aspects: (a) SR-rules are complex (many-to-many mappings), arbitrary and usually unknown beforehand; (b) decisions tendencies depend on previously evaluated feedbacks, so that conflict arises on the knowledge level; (c) errors are not induced by time pressure, but by cognitive difficulty; (d) conflicts could be diminished by mnemonic search; (e) feedback evaluation allows to improve performance in cognitive skills and knowledge. Exemplifying are paradigms like hypothesis testing [12], application of arbitrary SR-rules [24] or detection of arbitrary SR-rules [27,32]. Together, the critical feature of paradigms eliciting BA 8 activation seems to be the lack of means-end-related information, i.e., information about how

an initial state is transformed into a favorable final state. A situation in which the transformation of an initial state into a favorable goal state is hampered by a barrier is also referred to as a well-defined problem [11,29]. To successfully get over the barrier, one has to combine the target-oriented means in a so far unknown way. The process of solving well-defined problems is determined by two key features: difference reduction and sub-goaling [29]. Difference reduction refers to the tendency to select operators that produce states more similar to the goal state and sub-goaling to the interim states in this process. Sub-goal-achievement is indicated via feedback, which has to be evaluated in order to plan future target-oriented action steps.

In contrast, as soon as the requirement to transform an initial state into a goal state is obsolete and the specific correct action is pre-determined or can be retrieved from memory, the situation is conceived of as a well-defined task [1,11]. In this case, feedback information serves only as a reinsurance since the accomplishment of self-evident operations in a known way leads to the intended outcomes. Accordingly, paradigms, which reported BA 32/24 activation could be conceived of as well-defined tasks.

Together, the paradigmatic differentiation into ill- and well-defined decision problems is suggested to cause different activation patterns. In such a way that decisions which are uncertain because of insufficient means-end-related information elicit activation within mesial BA 8, whereas decisions which are uncertain because of insufficient inspection time elicit activation within BA 32/24. In sum, the processes investigated in Exps. 1 and 2 are suggested to draw rather on BA 8 than on BA 32/24 since the employed tasks correspond to the specific profile of well-defined decision problems. To put it shortly, we suggest activation within BA 8 and BA 32/24 may distinguish decision conflict from response conflict.

The present classification is not in conflict with the recent findings by Ridderinkhof et al. [42]. By means of a meta-analysis, the authors checked whether the posterior medial frontal cortex shows a differential involvement in sub-processes of performance monitoring. As a result, they did not find any support for this hypothesis. Rather, it revealed that an extensive part of the posterior medial frontal cortex – including BA 6, 8, 24 and 32 – showed to be activated, whereas, the most pronounced cluster of activation revealed within area 32. However, on the basis of our classification this finding is not unexpected, since 27 of 38 reviewed fMRI studies either used a Flankers task, go/no–go task, Stroop task and AX–CPT task or a combination of them. In contrast, the paradigms of five studies would have been ranked as well-defined decision problems according to our classification. Based on the schematic map by Ridderinkhof et al. [42] and the allocated coordinates, it revealed that all coordinates of the contrasts reported in these five studies fall into area 8. The remaining studies could not clearly be assigned to one of our two categories. Together, it remains to be tested whether the classification by Ridderinkhof and colleagues and ours can complement one another in order to reveal a differential involvement of the posterior medial frontal cortex or whether findings will support a disengagement from this assumption.

5.2. Attribution-dependent activation of uncertainty

Significant activations within the MFG, IFJ and IPS were found in the direct task contrast between internally and externally attributed uncertainty. The same sample of areas was found to increase with increasing internally attributed uncertainty (parametric effect) as well as in contrast to the control condition (main task effect). These results are taken to confirm the hypothesis that specifically knowledge uncertainty involves brain areas sub-serving WM functions.

The MFG (BA 46/9) is also referred to as mid-dorsolateral pre-frontal area [40]. Activations within this region have been reported when monitoring and manipulation of information within WM is required [10]. The monitoring of mnemonic information across trials as well as the manipulation of actively maintained information within WM is taken to be the key feature of tasks activating mid-dorsolateral pre-frontal areas [26,41] as in contrast to memory retrieval per se which has been shown to specifically activate the mid-ventrolateral pre-frontal cortex [33]. In Exp. 2, sustained monitoring and manipulation of feedback information across the experimental session was required so as to master the task successfully. Moreover, mnemonic information referred to SR-rules that were defined by different non-spatial object properties. The mid-dorso-lateral pre-frontal coordinates in the present study fit nicely to those reported for non-spatial WM in a recent meta-analysis by Owen [39] (Talairach coordinates right: 35, 32, 19; left: −42, 23, 19).

As typical for WM functions, posterior parietal areas were found to be co-activated in addition to MFG [39]. The former areas are taken to maintain all SR-rules that are valid in an experiment [7]. From this set, currently valid SR-rules are selected by corresponding pre-frontal sites [35]. In Exp. 2, it was required to represent all possible responses that were evoked by the task environment. Accordingly, posterior parietal areas are suggested to be involved in activating responses on the basis of SR-rules.

Considering activation within IFJ, there is evidence that this brain area is functionally separable from mid-dorsolateral and mid-ventrolateral pre-frontal cortex such that the IFJ sub-serves a function that could be described as the “updating of task representations”. Recent imaging studies showed that the implementation of learned SR-rules elicited activation within this area [2,36]. This interpretation can be applied to IFJ activation for knowledge uncertainty since the implementation and the updating of appropriate SR-rules is taken to be the key requirement in order to solve the task. Findings thereby confirm that memory search is an appropriate coping strategy with knowledge uncertainty.

Acknowledgments

We thank Andrea Gast-Sandmann for the stimulus material, Jennifer Kittel for assistance with data analysis, Karsten Mueller Andre Szameitat and Stefan Zysset for support in fMRI statistics. This work was supported by the German Research Foundation (SPP 1107).

Note: this manuscript combines results from two papers which were recently published in Neuroimage [52,53].

References

[1] S. Brander, A. Kompa, U. Peltzer, Denken und Problemlösen, Einführung in Die Kognitive Psychologie, Westdeutscher Verlag, Opladen, 1985.
[2] M. Brass, D.Y. von Cramon, The role of the frontal cortex in task preparation, Cereb. Cortex 12 (2002) 908–914.
[3] H.C. Breiter, I. Aharon, D. Kahneman, A. Dale, Functional imaging of neural responses to expectancy and experience of monetary gains and losses, Neuron 30 (2001) 619–639.
[4] D.V. Budescu, T.S. Wallsten, Subjective estimation of precise and vague uncertainties, in: G. Wright, P. Ayton (Eds.), Judgmental Forecasting, Wiley, Chichester, 1987, pp. 63–81.
[5] C. Büchel, A.P. Holmes, G. Rees, K.J. Friston, Characterizing stimulus–response functions using nonlinear regressors in parametric fMRI experiments, Neuroimage 8 (1998) 140–148.
[6] C. Büchel, R.J.S. Wise, C.J. Mummery, J.B. Poline, K.J. Friston, Nonlinear regression in parametric activation studies, Neuroimage 4 (1996) 60–66.
[7] S.A. Bunge, E. Hazeltine, M.D. Scanlon, A.C. Rosen, J.D.E. Gabrieli, Dissociable contributions of pre-frontal and parietal cortices to response selection, Neuroimage 17 (2002) 1562–1571.
[8] B.J. Casey, K.M. Thomas, T.F. Welsh, R.D. Badgaiyan, C.H. Eccard, J.R. Jennings, E.A. Crone, Dissociation of response conflict, attentional selection, and expectancy with functional magnetic resonance imaging, Proc. Natl. Acad. Sci. U.S.A. 97 (2000) 8728–8733.
[9] H.D. Critchley, C.J. Mathias, R.J. Dolan, Neural activity in the human brain relating to uncertainty and arousal during anticipation, Neuron 29 (2001) 537–545.
[10] M.D. D'Esposito, G.K. Aguirre, E. Zarahn, D. Ballard, R.K. Shin, J. Lease, Functional MRI studies of spatial and nonspatial working memory, Cogn. Brain Res. 7 (1998) 1–13.
[11] D. Dörner, H.W. Kreuzig, F. Reither, T. Stäudel, Vom Umgang Mit Unbestimmtheit und Komplexität, Huber, Bern, 1983.
[12] R. Elliott, R.J. Dolan, Activation of different anterior cingulate foci in association with hypothesis testing and response selection, Neuroimage 8 (1998) 17–29.
[13] R. Elliott, C.D. Frith, R.J. Dolan, Differential neural responses to positive and negative feedback in planning and guessing tasks, Neuropsychologia 35 (1997) 1395–1404.
[15] R. Elliott, G. Rees, R.J. Dolan, Ventromedial pre-frontal cortex mediates guessing, Neuropsychologia 37 (1999) 403–411.
[16] C. Fassbender, R. Hester, H. Garavan, A review of midline activations associated with error processing and conflict monitoring, Neuroimage 19 (2003) 393.
[17] P.C. Fletcher, R.N.A. Henson, Frontal lobes and human memory, Brain 124 (2001) 849–881.
[18] K.J. Friston, Statistical parametric mapping, in: R.W. Thatcher, M. Hallet, T. Zeffiro, E.R. John, M. Huerta (Eds.), Functional Neuroimaging: Technical Foundations, Academic Press, San Diego, 1994, pp. 79–93.
[19] K.J. Friston, A.P. Holmes, J.B. Poline, P.J. Grasby, S.C. Williams, R.S. Frackowiak, R. Turner, Analysis of fMRI time-series revisited, Neuroimage 2 (1995) 45–53.
[20] K.J. Friston, P. Fletcher, O. Josephs, A. Holmes, M.D. Rugg, R. Turner, Event-related fMRI: characterizing differential responses, Neuroimage 7 (1998) 30–40.
[21] H. Garavan, T.J. Ross, K. Murphy, R.A.P. Roche, E.A. Stein, Dissociable executive functions in the dynamic control of behavior: inhibition, error detection, and correction, Neuroimage 17 (2002) 1820–1829.
[22] H. Garavan, T.J. Ross, J. Kaufman, E.A. Stein, A midline dissociation between error-processing and response–conflict monitoring, Neuroimage 20 (2003) 1132–1139.
[23] P.W. Glimcher, A. Rustichini, Neuroeconomics: the consilience of brain and decision, Science 306 (2004) 447–452.
[24] V. Goel, R.J. Dolan, Anatomical segregation of component processes in an inductive inference task, J. Cogn. Neurosci. 12 (2000) 110–119.
[25] V. Goel, B. Gold, S. Kapur, S. Houle, The seats of reason? An imaging study of deductive and inductive reasoning, Neuroreport 8 (1997) 1305–1310.
[26] A.A. Hartley, N.K. Speer, Locating and fractionating working memory using functional magnetic resonance imaging: storage, maintenance, and executive functions, Microsc. Res. Tech. 51 (2000) 45–53.
[27] C.B. Holroyd, S. Nieuwenhuis, N. Yeung, L. Nystrom, R.B. Mars, M.G.H. Coles, J.D. Cohen, Dorsal anterior cingulate cortex shows fMRI response to internal and external error signal, Nat. Neurosci. 7 (2004) 497–498.
[28] W.C. Howell, Uncertainty from internal and external sources: a clear case of overconfidence, J. Exp. Psychol. 89 (1971) 240–243.
[29] N. Jausovec, K. Jausovec, EEG activity during the performance of complex mental problems, Int. J. Psychophysiol. 36 (2000) 73–88.
[30] D. Kahneman, A. Tversky, Variants of uncertainty, Cognition 11 (1982) 143–157.
[31] J.G. Kerns, J.D. Cohen, A.W. MacDonald III, R.Y. Cho, V.A. Stenger, C.S. Carter, Anterior cingulate conflict monitoring and adjustments in control, Science 303 (2004) 1023–1026.
[32] B. Knutson, G.W. Fong, S.M. Bennett, C.M. Adams, D. Hommer, A region of mesial pre-frontal cortex tracks monetarily rewarding outcomes: characterization with rapid event-related fMRI, Neuroimage 18 (2003) 263–272.
[33] P. Kostopoulos, M. Petrides, The mid-ventrolateral pre-frontal cortex: insights into its role in memory retrieval, Eur. J. Neurosci. 17 (2003) 1489–1497.
[34] G. Lohmann, K. Mueller, V. Bosch, H. Mentzel, S. Hessler, L. Chen, D.Y. von Cramon, Lipsia: a new software system for the evaluation of functional magnetic resonance images of the human brain, Comput. Med. Imaging Graph. 25 (2001) 449–457.
[35] E.K. Miller, J.D. Cohen, An integrative theory of pre-frontal cortex function, Annu. Rev. Neurosci. 24 (2001) 167–2002.
[36] Y. Nagahama, T. Okada, Y. Katsumi, T. Hayashi, H. Yamauchi, C. Oyanagi, J. Konishi, H. Fukuyama, H. Shibasaki, Dissociable mechanisms of attentional control within the human pre-frontal cortex, Cereb. Cortex 11 (2001) 85–92.
[37] D.G. Norris, S. Zysset, T. Mildner, C.J. Wiggins, An investigation of the value of spin-echo-based fMRI using a Stroop color–word matching task and EPI at 3T, Neuroimage 15 (2002) 719–726.
[38] J.O. O'Doherty, M.I. Kringelbach, E.T. Rolls, J. Hornak, C. Andrews, Abstract reward and punishment representations in the human orbito-frontal cortex, Nat. Neurosci. 4 (2001) 95–102.
[39] A.M. Owen, The role of the lateral frontal cortex in mnemonic processing: the contribution of functional neuroimaging, Exp. Brain Res. 133 (2000) 33–43.
[40] M. Petrides, The role of the mid-ventrolateral pre-frontal cortex in working memory, Exp. Brain Res. 133 (2000) 44–54.
[41] M. Petrides, The mid-ventrolateral pre-frontal cortex and active mnemonic retrieval, Neurobiol. Learn. Mem. 78 (2002) 528–538.
[42] K.R. Ridderinkhof, M. Ullsperger, E.A. Crone, S. Nieuwenhuis, The role of the medial frontal cortex in cognitive control, Science 306 (2004) 443–447.

[43] R.D. Rogers, A.M. Owen, H.C. Middelton, E.J. Williams, J.D. Pickard, B.J. Sahakian, T.W. Robbins, Choosing between small, likely rewards and large, unlikely rewards activates inferior and orbital pre-frontal cortex, J. Neurosci. 20 (1999) 9029–9038.
[44] K. Rubia, A.B. Smith, M.J. Brammer, E. Taylor, Right inferior prefrontal cortex mediates response inhibition while mesial pre-frontal cortex is responsible for error detection, Neuroimage 20 (2003) 351–358.
[45] C.C. Ruff, T.S. Woodward, K.R. Laurens, P.F. Liddle, The role of the anterior cingulate cortex in conflict processing: evidence from reverse Stroop interference, Neuroimage 14 (2001) 1150–1158.
[46] R.I. Schubotz, D.Y. von Cramon, A blueprint for target motion: fMRI reveals perceptual complexity to modulate a premotor-parietal network, Neuroimage 16 (2002) 920–935.
[47] P. Talairach, J. Tournoux, A Stereotactic Coplanar Atlas of the Human Brain, Thieme, Stuttgart, 1988.
[48] K.H. Teigen, Variants of subjective probabilities: concepts, norms, and biases, in: G. Wright, P. Ayton (Eds.), Subjective Probability, Wiley, Chichester, 1994, pp. 211–238.
[49] M. Ullsperger, D.Y. von Cramon, Subprocesses of performance monitoring: a dissociation of error processing and response competition revealed by event-related fMRI and ERP's, Neuroimage 14 (2001) 1387–1401.
[50] M. Ullsperger, D.Y. von Cramon, Error monitoring using external feedback: specific roles of the habenular complex, the reward system, and the cingulate motor area revealed by functional magnetic resonance imaging, J. Neurosci. 23 (2003) 4308–4314.
[51] V. van Veen, J.D. Cohen, M.M. Botvinick, V.A. Stenger, C.S. Carter, Anterior cingulate cortex, conflict monitoring, and levels of processing, Neuroimage 14 (2001) 1302–1308.
[52] K.G. Volz, R.I. Schubotz, D.Y. von Cramon, Predicting events of varying probability: uncertainty investigated by fMRI, Neuroimage 19 (2003) 271–280.
[53] K.G. Volz, R.I. Schubotz, D.Y. von Cramon, Why am I unsure? Internal and external attributions of uncertainty dissociated by fMRI, Neuroimage 21 (2004) 848–857.
[55] K.J. Worsley, K.J. Friston, Analysis of fMRI time-series revisited again, Neuroimage 2 (1995) 173–181.